We are IntechOpen,
the world's leading publisher of
Open Access books
Built by scientists, for scientists

6,900
Open access books available

186,000
International authors and editors

200M
Downloads

Our authors are among the

154
Countries delivered to

TOP 1%
most cited scientists

12.2%
Contributors from top 500 universities

CLARIVATE ANALYTICS
BOOK CITATION INDEX
INDEXED

WEB OF SCIENCE™

Selection of our books indexed in the Book Citation Index
in Web of Science™ Core Collection (BKCI)

Interested in publishing with us?
Contact book.department@intechopen.com

Numbers displayed above are based on latest data collected.
For more information visit www.intechopen.com

Optical Network Optimization Based on Particle Swarm Intelligence

Fábio Renan Durand, Larissa Melo,
Lucas Ricken Garcia, Alysson José dos Santos and
Taufik Abrão

Additional information is available at the end of the chapter

1. Introduction

Modern optical communication networks are expected to meet a broad range of services with different and variable demands of bit rate, connection (session) duration, frequency of use, and set up time [1]. Thus, it is necessary to build flexible all-optical networks that allow dynamic resources sharing between different users and clients in an efficient way. The all-optical network is able to implement ultrahigh speed transmitting, routing and switching of data in the optical domain, presenting the transparency to data formats and protocols which increases network flexibility and functionality such that future network requirements can be met [2]. Optical code division multiplexing access (OCDMA) based technology has attracted a lot of interests due to its various advantages including asynchronous operation, high network flexibility, protocol transparency, simplified network control and potentially enhanced security [3]. Therefore, recent developments and researches on OCDMA have been experienced an expansion of interest, from short-range networks, such as access networks, to high-capacity medium/large networks.

The optical network presents two promising scenarios: the transport (backbone) networks with optical code division multiplexing/wavelength division multiplexing (OCDM/WDM) technology and the access network with OCDMA technology. In both, transport OCDM/WDM and access OCDMA networks, each different code defines a specific user or logic channel transmitted in a common channel. In a common channel, the interference that may arise between different user codes is known as multiple access interference (MAI), and it can limit the number of users utilizing the channel simultaneously [3]. In this work we

INTECH
open science | open minds

have focus on hybrid OCDM/WDM systems. In this one, data signals in routing network configuration are carried on optical code path (OCP) from a source node to a destination node passing through nodes where the signals are optically routed and switched without regeneration in the electrical domain. Hence, in routing and channel (code/wavelength) assignment (RCA) problem, suitable paths and channels are carefully selected among the many possible choices for the required connections [2].

Establishing OCP with higher optical signal-to-noise plus interference ratio (SNIR) allows reducing the number of retransmissions by higher layers, thus increasing network throughput. Therefore, RCA techniques that consider physical layer impairments for the establishment of an OCP, namely Quality of Transmission-Aware (QoT-aware) RCA, could be much more practical [4-5]. For a dynamic traffic scenario the objective is to minimize the blocking probability of the connections by routing, assigning channels, and to maintain an acceptable level of optical power and adequate SNIR all over the network [6]. Furthermore, different channels can travel via different optical paths and also have different levels of quality of service (QoS) requirements. The QoS depends on SNIR, dispersion, and nonlinear effects [6]. Therefore, it is desirable to adjust network parameters in an optimal way, based on on-line decentralized iterative algorithms to accomplish such adjustment [7].

As a result, this dynamic optimization allows an increased network flexibility and capacity [6-7]. The SNIR optimization problem appears to be a huge challenge, since the MAI introduces the near-far problem [7]. Furthermore, if the distances between the nodes are quite different, like in real optical networks, the signal power received from various nodes will be significantly distinct. Thus, considering an optical node as the reference, the performance of closer nodes is many orders of magnitude better than that of far ones. Then, an efficient power control is needed to overcome this problem and enhance the performance and throughput of the network; this could be achieved through the SNIR optimization [6]. In this case, which is analogous to the CDMA cellular system, the power control (centralized or distributed) is one of the most important issues, because it has a significant impact on both network performance and capacity. It is the most effective way to avoid the near-far problem and to increase the SNIR [6-7].

The optical power control problem has been recently investigated in the context of access networks aiming at solving the near-far problem [7-8] and establishing the QoS at the physical layer [9-11]. In [7], the impact of power control on the random access protocol was investigated. In [8], the effect of near-far problem and a detailed review of the power control were presented including the use of distributed algorithms. On the other hand, in [9-12] the concept that users of various classes should transmit at different power levels was applied. Distinct power levels were obtained with power attenuators [10], adjustable encoders/decoders [11], and adjustable transmitters [12]. Furthermore, the optimal selection of the system's parameters such as the transmitted power and the information rate would improve their performances [9, 13-15]. In [13], optical power control and time hopping for multimedia applications using single wavelength was proposed. The approach accommodates various data rates using only one sequence by changing the time-hopping rate. However, in order to implement such system an optical selector device that consists of a number of optical hard-

limiters is needed [13]. On the other hand, in [14] a multi rate and multi power level scheme using adaptive overlapping pulse-position modulator (OPPM) and optical power controller was proposed. The bit rate varies depending on the number of slots in the optical OPPM system and has the advantage that it is not required to change the code sequence depending on the required user's information rate. The power level can be achieved by accommodating users with the different transmitted power. The power controller requires only power attenuator, and the difference of the power does not cause the change of the bit rate. In [15] a hybrid power and rate control nonlinear programming algorithm for overlapped optical fast frequency hopping (OFFH) was proposed. The multi rate transmission is achieved by overlapping consecutive bits while coded using fiber Bragg grating (FBG). The intensity of the transmitted optical signal is directly adjusted from the laser source with respect to the transmission data rate. The proposed algorithm provides a joint transmission power and overlapping coefficient allocation strategy, which has been obtained via the solution of a constrained optimization problem, which maximizes the aggregate system throughput subject to a peak laser transmission power constraint. In [9], a control algorithm to solve the unfairness in the resource allocation strategy presented in [10] has been analyzed. Also, a unified framework for allocating and controlling the transmission rate and power in a way that it can be applied for any expression of the system capacity was implemented.

Besides, recently researches have showed the utilization of resource allocation and optimization algorithms such as Local Search, Simulated Annealing, GA, Particle Swarm optimization (PSO), Ant Colony optimization (ACO) and Game Theory to regulate the transmitted power, bit rate variation and the number of active users in order to maximize the aggregate throughput of the optical networks [16-17]. However, the complexity and unfairness in the strategies presented are aspects to be improved. On the other hand, resource allocation has not been largely investigated considering energy efficiency aspects. This issue has become paramount since energy consumption is dominated by the access segment due to the large amount of distributed network elements. The related works have showed the utilization of resource allocation and optimization algorithms to optimization of the access network; however, these issues have not been largely investigated considering routed OCDM/WDM networks [6]. In the case of the OCP networks optimization, it is necessary to consider the use of distributed iterative algorithms with high performance-complexity tradeoffs and the imperfections of physical layer, which constitute a new research area so far, which was investigated under an analytical perspective in [6].

It is worth noting the routed OCDM/WDM networks brings a new combination of challenges with the power control, like amplified spans, multiple links, accumulation, and self-generation of the optical spontaneous noise power (ASE) noise, as well as the MAI generated by the OCPs. On the other hand, the dispersive effects, such as chromatic or group velocity dispersion (GVD) and polarization mode dispersion (PMD), are signal degradation mechanisms that significantly affect the overall performance of optical communication systems [6, 18-21].

In this chapter, optimization procedures based on PSO are investigated in details, aiming to efficiently solve the optimal resource allocation for SNIR optimization of OCPs from OCDM/WDM networks under QoS restrictions and energy efficiency constraint problem,

considering imperfections on physical constraints. Herein, the adopted SNIR model considers the MAI between the OCP based on 2-D codes (time/wavelength) [22, 23], ASE at cascaded amplified spans, and GVD and PMD dispersion effects.

The optimization method based on the heuristic PSO approach is attractive due to its performance-complexity tradeoff and fairness features regarding the optimization methods that deploy matrix inversion, purely numerical procedures and other heuristic approaches [9][17].

The chapter is organized in the following manner: in Section 2 the optical transport (OCDM/WDM) is described, while in Section 3 the SNIR optimization for the OCPs based on particle swarm intelligence is described in order to solve the resource allocation problem. In the network optimization context, figures of merit are presented and the PSO is developed in Section 4, with emphasis on its input parameters optimal choice and the network performance. Afterward, numerical results are discussed for realistic networks operation scenarios. Finally, the main conclusions are offered in Section 5.

2. Network architecture

2.1. OCDM/WDM transport network

The transport network considered in this work is formed by nodes that have optical core routers interconnected by OCDM/WDM links with optical code paths defined by patterns of short pulses in wavelengths, such as shown in Fig. 1. The links are composed by sequences of span and each span consists of optical fiber and optical amplifier. The transmitting and receiving nodes create virtual path based on the code and the total link length is given by $d_{ij} = \sum_i d_i^{tx} + \sum_j d_j^{rx}$, where d_i^{tx} is the span length from the transmitting node to the optical router and d_j^{rx} is the span between optical routers in the OCP route and the receiving node. The received power at the j-th node is given by $P_r = a_{star} p_i G_{amp} \exp(-\alpha_f d_{ij})$, where p_i is the transmitted power by the i-th transmitter node, α_f is the fiber attenuation (km^{-1}) and a_{star} is the star coupler attenuation (linear units), and G_{amp} is the total gain at the route. Considering decibel units, $a_{star} = 10\log(K) - [10\log_2(K)\log_{10}\delta]$, where, δ is the excess loss ratio [6]. A typical distance between optical amplifiers is about 60 km [20].

The optical core router consists of code converter routers in parallel forming a two-dimensional router node [23] and each group of code converters in parallel is pre-connected to a specific output performing routing by selecting a specific code from the incoming broadcasting traffic. This kind of router does not require light sources or optical-electrical-optical conversion and can be scaled by adding new modules [22]. This code is transmitted and its route in the network is determined by a particular code sequence. For viability characteristics, we consider network equipment, such as code-processing devices (encoders and decoders at the transmitter and receiver), star coupler, optical routers could be made using robust, lightweight, and low-cost technology platforms with commercial-off-the-shelf technologies [23-24]. For more details about transport networks the references [19],[25] should be consulted.
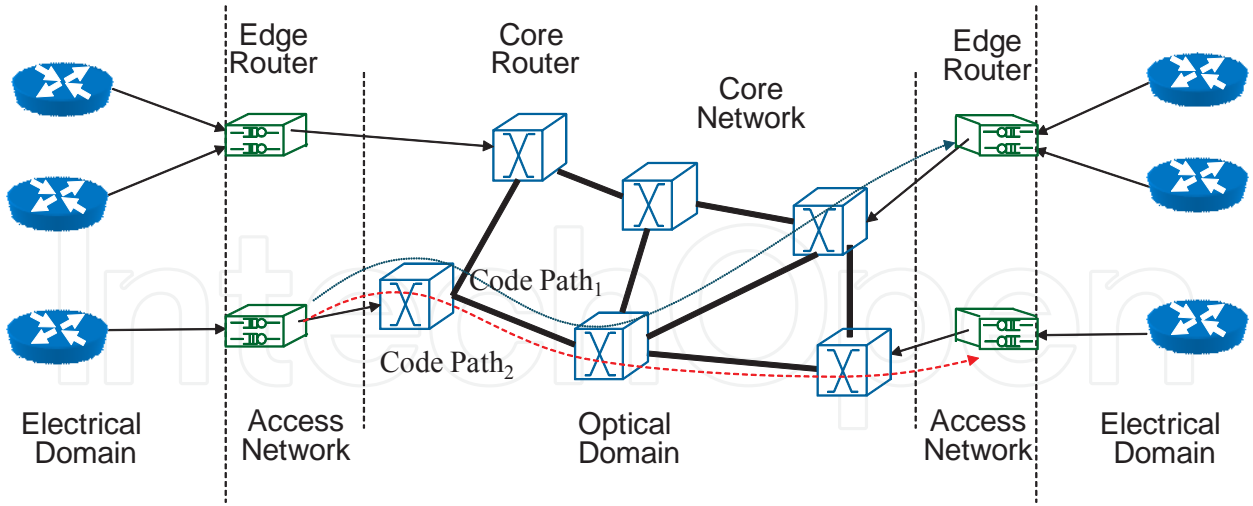
Figure 1. OCDM/WDM routed network architecture.

2.2. OCDMA codes

The OCDMA can be divided into a) non-coherent unipolar systems, based only on optical power intensity modulation [20], and b) coherent bipolar systems, based on amplitude and phase modulation [26]. As expected, the performance of coherent codes is higher than that of non-coherent ones when analyzing the SNIR [27]. This effect occurs, because the bipolar code is true-orthogonal, and the unipolar code is pseudo-orthogonal. However, the main drawback to the coherent OCDMA lies in the technical implementation difficulties, concomitant with the utilization of phase-shifted optical signals [20],[27]. In this work we adopt non-coherent codes because their technological maturity and implementation easiness when compared with coherent codes [28]. The non-coherent codes can be classified into one-dimensional (1-D) and two-dimensional (2-D) codes. In the 1-D codes, the bits are subdivided in time into many short chips with a designated chip pattern representing a user code. On the other hand, in the 2-D codes, the bits are subdivided into individual time chips, and each chip is assigned to an independent wavelength out of a discrete set of wavelengths. The 2-D codes have better performance than the 1-D codes, and they can significantly enhance the number of active users [29]. Besides, the 2-D codes have been applied only in access networks [2]; in this way, recently the utilization of the 2-D codes to obtain optical code path routed networks was proposed, which performance evaluated by simulation, considering coding, topology, load condition, and physical impairment [2][6][20][21][22].

The 2-D codes can be represented by $N_\lambda \times N_T$ matrices, where N_λ is the number of rows, that is equal to the number of available wavelengths, and N_T is the number of columns, that is equal to the code length. The code length is determined by the bit period T_B which is subdivided into small units namely chips, each of duration $T_c = T_B / N_T$, as show Fig. 2(a). In each code, there are w short pulses of different wavelength, where w is called the weight of the code. An $(N_\lambda \times N_T, w, \lambda_a, \lambda_c)$ code is the collection of binary $N_\lambda \times N_T$ matrices each of code weight w; the parameters λ_a and λ_c are nonnegative integers and represent the constraints

on the 2-D codes autocorrelation and cross-correlation, respectively [3]. The 2-D code design and selection is very important for good system performance and high network scalability with low bit error rate (BER). In [3] and [28] is presented an extensive list of code construction techniques, as well as their technological characteristics are discussed.

The OCDMA 2-D encoder creates a combination of two patterns: a wavelength-hopping pattern and a time-spreading pattern. The common technology applied for code encoders/ decoders fiber Bragg gratings (FBGs), as show Fig. 2(b). The losses associated with the encoders/ decoders are given by $C_{Bragg}(dB) = N_{\lambda} a_{Bragg} + a_{Circulator}$ [22], where a_{Bragg} is the FBG loss and $a_{Circulator}$ is the circulator loss. The usual value of losses for these equipments are a_{Bragg} = 0.5 dB and $a_{Circulator}$ = 3dB.
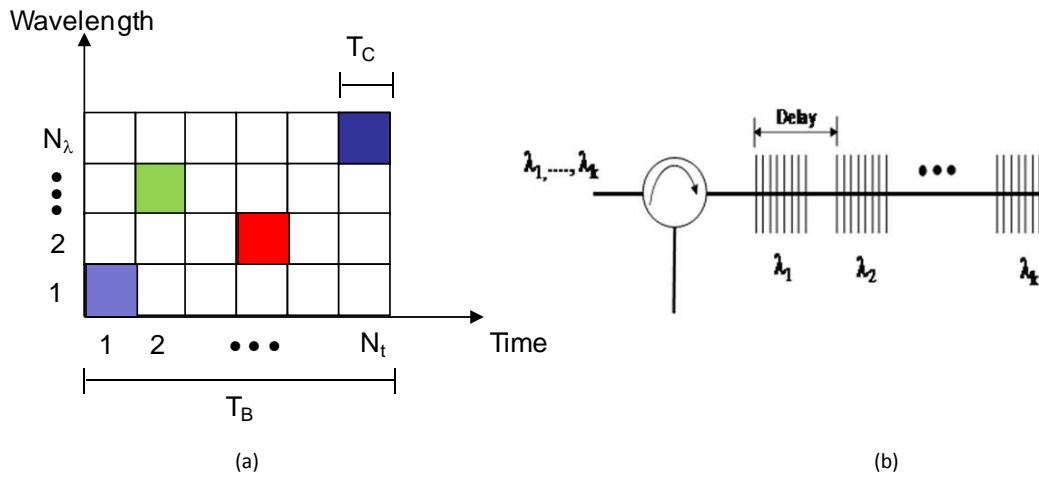

Figure 2. a) Representation of optical OCDMA codes. (b) Schematic of 2-D encoders/decoders based on fiber Bragg gratings (FBGs).

3. SNIR optimization procedures

In the present approach, the SNIR optimization is based on the definition of the minimum power constraint (also called sensitivity level) assuring that the optical signal can be detected by all optical devices. The maximum power constraint guarantees the minimization of nonlinear physical impairments, because it makes the aggregate power on a link to be limited to a maximum value. The power control in optical networks appears to be an optimization problem.

3.1. Problem description

Denoting Γ_i the carrier-to-interference ratio (CIR) at the required decoder input, in order to get a certain maximum bit error rate (BER) tolerated by the *i-th* optical node, and defining the *K*-dimensional column vector of the transmitted optical power p = $[p_1, p_2,..., p_K]^T$, the optical power control problem consists in finding the optical power vector p that minimizes the cost function $J(p)$ can be formulated as [6],[8] :

$$\min_{\mathbf{p}\in\mathbb{R}_+^K} J(\mathbf{p}) = \min_{\mathbf{p}\in\mathbb{R}_+^K} \mathbf{1}^T \mathbf{p} = \min_{p_i\in\mathbb{R}_+} \sum_{i=1}^{K} p_i,$$

$$subject\ to : \Gamma_i = \frac{\left(G_{ii}p_i G_{amp}\right)/\sigma_D}{G_{amp}\sum\limits_{j=1,j\neq i}^{K} G_{ij}p_j + 2N_{sp}^{eq}} \geq \Gamma^*$$

$$P_{\min} \leq p_i \leq P_{\max} \ \forall i = 1,..,K,$$

$$P_{\min} \geq 0, \quad P_{\max} > 0$$

$$(1)$$

where $1^T = [1,..., 1]$ and Γ^* is the minimum CIR to achieve a desired QoS; G_{ii} is the attenuation of the OCP taking into account the power loss between the nodes, according to network topology, while G_{ij} corresponds to the attenuation factor for the interfering OCP signals at the same route, G_{amp} is the total gain at the OCP, N_{sp}^{eq} is the spontaneous noise power (ASE) for each polarization at cascaded amplified spans [29], p_i is the transmitted power for the i-OCP and p_j is the transmitted power for the interfering OCP; σ_D is the pulse spreading due to the combined effects of the GVD and the first-order PMD for Gaussian pulses [30]. Using matrix notations, (1) can be written as $[I - \Gamma^* H]p \geq u$, where I is the identity matrix, H is the normalized interference matrix, which elements evaluated by $H_{ij} = G_{ij}/G_{ii}$ for $i \neq j$ and zero for another case, thus $u_i = \Gamma^* N_{sp}^{eq}/G_{ii}$, where there is a scaled version of the noise power. Substituting inequality by equality, the optimized power vector solution through the matrix inversion $p^* = [I - \Gamma^* H]^{-1}u$ could be obtained. The matrix inversion is equivalent to centralized power control, i.e. the existence of a central node in power control. The central node stores information about all physical network architecture, such as fiber length between nodes, amplifier position and regular update for the OCP establishment, and traffic dynamics. These observations justify the need for on-line SNIR optimization algorithms, which have provable convergence properties for general network configurations [6, 16, 29].

The SNIR and the carrier to interference ratio in eq. (1) are related to the factor N_T/σ, i. e., $\gamma_i \approx (N_T/\sigma)^2 \Gamma_i$. The bit error probability (BER) is given by $P_b(i) = erfc\left(\sqrt{\gamma_i}/2\right)/2$, when the Gaussian approximation is adopted, and the signal-to-noise plus interference ratio (SNIR) at each OCP, considering the 2-D codes, is given by [6, 8],

$$\gamma_i = \frac{N_T^2\left(G_{ii}p_i G_{amp}\right)/\sigma_D}{\sigma^2 G_{amp}\sum\limits_{j=1,j\neq i}^{K} G_{ij}p_j + 2N_{sp}^{eq}}$$

$$(2)$$

where the average variance of the Hamming aperiodic cross-correlation amplitude is represented by σ^2 [3].

3.2. Physical restrictions

The physical impairments are signal degradation mechanisms that significantly affect the overall performance of optical communication systems [6]. For the data that are transmitted through a transparent optical network, degradation effects may accumulate over a large distance. The major linear physical impairments are group velocity dispersion (GVD), polarization mode dispersion (PMD), and amplifier spontaneous emission (ASE) noise [24]. On the other hand, the major nonlinear physical impairments are self phase modulation (SPM), cross-phase modulation (XPM), and four wave mixing (FWM), stimulated Brillouin scattering (SBS), and Raman scattering (SRS). The nonlinear physical impairments are excited with high power level [24]. However, the maximum power constraint guarantees the minimization of nonlinear physical impairments, because it makes the aggregate power on a link to be limited to a maximum value [6]. In the currently technology stage, besides GVD, the main linear impairment is the PMD, that must be considered in high capacity optical networks. Differently from GVD, PMD is usually difficult to accurately determine and compensate due to its dynamic nature and its fluctuations induced by external stress/strain applied to the fiber after installation [5] [21][22]. As a result, the signals quality in an OCDM/WDM network can be quickly evaluated by analyzing the GVD, PMD and MAI restrictions. PMD impairment establishes an upper bound on the length of the optical segment due to fiber dispersion which causes the temporal spreading of optical pulses. On the other hand, due to the advances in the fiber manufacturing process with a continuous reduction of the PMD parameter, the deleterious effect of PMD will not be an issue for 10 Gbps or lower bit rates, for future small and medium-sized networks [20] [21]. In this context, the dominant impairment in SNIR will be given by i) ASE noise accumulation in chains of optical amplifiers for future optical networks [29] and ii) ASE, GVD and PMD for currently stage of optical networks.

The dispersive effects, such as chromatic or group velocity dispersion (GVD) and polarization mode dispersion (PMD) constitute degradation mechanisms of the optical signal that significantly affect the overall performance of optical communication systems [21]. Currently, the PMD effect appears to be the only major physical impairment that must be considered in high capacity optical networks, which can hardly be controlled due to its dynamic and stochastic nature [5][21-22]. On the other hand, the GVD causes the temporal spreading of optical pulses that limits the product line rate and link length [6-30]. The pulse spreading effect due to the combined effects of the GVD and the first-order PMD for Gaussian pulses can be calculated as [30]:

$$\sigma_D = \left\{ \left(1 + \frac{C_p \beta_2 d_{ij}}{2\tau_0^2} \right) + \left(\frac{\beta_2 d_{ij}}{2\tau_0^2} \right) + x - \left(\frac{1}{2(1 + C_p^2)} \times \sqrt{1 + \frac{4}{3}(1 + C_p^2)x} - 1 \right) \right\}^{1/2} \tag{3}$$

where C_p is the chirp parameter, $\tau_0 = \dfrac{T_C}{2\sqrt{2\ln 2}}$ is the RMS pulse width, T_c is the chip period at half maximum, $\beta_2 = -D\lambda_0^2 / 2\pi c$ is the GVD factor, D is the dispersion parameter, c is the speed of light in the vacuum, $x = \Delta\tau^2 / 4\tau_0^2$ and $\Delta\tau = D_{PMD}\sqrt{d_{ij}}$, D_{PMD} is the PMD parameter,

and d_{ij} is the link length. Although there is a difference in the GVD for each wavelength, resulting from time skewing between the wavelengths, the consideration of the same GVD value for the entire transmission window is reasonable for a small number of wavelengths, as for the present code [27], [28]. On the other hand, this approximation is utilized to obtain an analytical treatment of the GVD and the PMD, in the same and less complex formalism, rather than to apply a formalism based on numerical methods [6].

The ASE (N_{sp}^{eq}) at the cascaded amplified spans is given by the model presented in Fig. 3 [29].
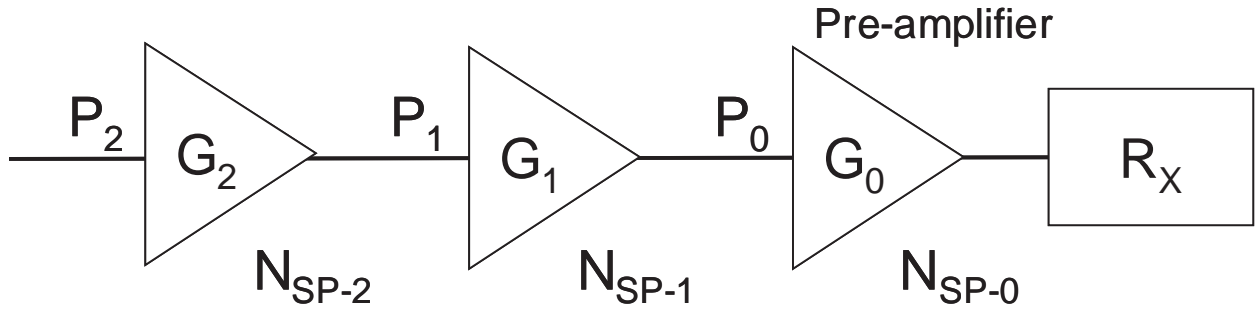

Figure 3. Cascading amplifiers.

This model considers that the receiver gets the signal from a link with cascading amplifiers, numbered as 1, 2,.., starting from the receiver. The pre-amplifier can be contemplated as the number 0 cascade amplifier. Let G_i be the amplifier gain, i. e. N_{sp}-i will be its spontaneous emission factor. The span between the i-*th* and the (*i − 1*)-*th* amplifier has the attenuation G_{ii}. Let P_{ti} be the mark power at the *i-th* amplifier input. The equivalent spontaneous emission factor is given by [24], [29]

$$N_{sp}^{eq} = \frac{N_{sp-1}(G_1 - 1)G_{ii}G_0 + N_{sp-0}(G_0 - 1)}{G_1 G_{ii} G_0 - 1} \tag{4}$$

Calculating recursively the N_{sp}^{eq} factor, one can find the noise at the cascading amplifiers. The noise for i-*th* amplifier is given by $N_{sp-i} = 2n_{sp}hf(G_i - 1)B_0$, which take into account the two polarization mode presented in a single mode fiber [24]. Where n_{sp} is the spontaneous emission factor, typically around 2 − 5, h is Planck's constant, f is the carrier frequency, G_i is the amplifier gain and *Bo* is the optical bandwidth. Ideally, to reduce the ASE noise power, the optical bandwidth can be set to a minimum of *Bo* = 2*R*, where *R* is the bit rate. Without loss of generality, all employed optical amplifiers provide a uniform gain, setting the maximum obtainable Erbium-doped fiber amplifier (EDFA) to 20 dB across the transmission window. This is a reasonable assumption for the reduced number of wavelengths in the code transmission window (4 wavelengths), considering the optical amplifier gain profile, where the

maximum difference of this gain is 0.4 dB for the wavelength, which is the most distant one from the central wavelength (1550 nm), with spectral spacing of 100 GHz [6][17].

3.3. Particle swarm optimization

3.3.1. PSO description

Particle Swarm Optimization (PSO) is a population-based stochastic optimization algorithm for global optimization that was presented first in 1995 [31]. It is based on the behavior of social groups like fish schools or bird flocks and it differs from other well-known Evolution-ary Algorithms (EA). As in EA, a population of potential solutions is used to probe the search space, but no operators, inspired by evolution procedures, are applied on the popula-tion to generate new promising solutions [32]. The fact which is recursively exploited is that an improved performance can be gained by interactions between individuals, or more spe-cifically by imitation of successful individuals. In a PSO system, particles fly around in mul-tidimensional search space. During the flight, each particle adjusts its position according to its own experience, and the experience of neighboring particles, making use of the best posi-tion encountered by itself and its neighbors. The swarm direction of a particle is defined by the set of particles neighboring the particle and its history experience. Although PSO does not rely on the survival of the fittest principle, it is often classified as an evolutionary algo-rithm (EA) because the update equations, which control the movement of individuals, are similar to the evolutionary operators used in EAs.

In general, the PSO performance for resource allocation problem can guarantee fast conver-gence and fairness within fewer iterations regarding the genetic algorithm-based [16]. It is well known in the literature that the PSO performance for resource allocation problem is highly dependent on its control parameters and that recommended parameter settings from the literature often do not lead to reliable and fast convergence behavior for the considered optimization problem [33], [34], [35].

In the PSO process, each particle keeps track of its coordinates in the space of interest, which are associated with the best solution (fitness) it has achieved so far. Another best value tracked by the global version of the particle swarm optimizer is the overall best value, and its location, obtained so far by any particle in the population. At each time iteration step, the PSO concept consists of velocity changes of each particle toward local and global locations. Acceleration is weighted by a random term, with separate random numbers being generated for acceleration toward local and global locations. Let b_p and v_p denote a particle coordinates (position) and its corresponding flight speed (velocity) in a search space, respectively. In this strategy, each power-vector candidate $\mathbf{b}_p[t]$, with dimension $K \times 1$, is used for the velocity-vector calculation of the next iteration [33]:

$$\mathbf{v}_p[t+1] = \omega[t] \bullet \mathbf{v}_p[t] + C_1 \bullet \mathbf{U}_{p1}[t]\left(\mathbf{b}_p^{best}[t] - \mathbf{b}_p[t]\right) + C_2 \quad \bullet \mathbf{U}_{p2}[t]\left(\mathbf{b}_g^{best}[t] - \mathbf{b}_p[t]\right) \tag{5}$$

where $\omega[t]$ is the inertia weight of the previous velocity in the present speed calculation, the velocity-vector has K dimension $\mathbf{v}_p[t]=[\mathrm{v}_{p1}^t\,\mathrm{v}_{p2}^t\,\dots\,\mathrm{v}_{pK}^t]^T$; the diagonal matrices $\mathbf{U}_{p1}[t]$ and $\mathbf{U}_{p2}[t]$ with dimension K have their elements as random variables with uniform distribution $\sim U \in [0, 1]$, generated for the pth particle at iteration $t = 1, 2,..., \mathsf{G}$; $\mathbf{b}_g^{best}[t]$ and $\mathbf{b}_p^{best}[t]$ are the best global vector-position and the best local vector-position found until the t_{th} iteration, respectively; C_1 and C_2 are acceleration coefficients regarding the best particles and the best global positions influences in the velocity updating, respectively. The p_{th} particle's position at the tth iteration is defined by the power candidate-vector $\mathbf{b}_p[t]=[\mathrm{b}_{p1}^t\,\mathrm{b}_{p2}^t\,\dots\,\mathrm{b}_{pK}^t]^T$. The position of each particle is updated using the new velocity vector for that particle,

$$\mathbf{b}_p[t+1]=\mathbf{b}_p[t]+\mathbf{v}_p[t+1], \quad p=1, \ \dots, \ \mathsf{P} \tag{6}$$

where P is the population size. In order to reduce the likelihood that the particle might leave the search universe, maximum velocity factor V_{max} factor is added to the PSO model, which will be responsible for limiting the velocity to the range $[\pm V_{max}]$. Hence, the adjustment of velocity allows the particle to move in a continuous but constrained subspace, been simply accomplished by:

$$\mathrm{v}_{pk}^t=\min\{V_{max}; \max\{-V_{max}; \mathrm{v}_{pk}^t\}\}, \quad k=1, \ \dots, \ K; \ p=1, \ \dots, \ \mathsf{P} \tag{7}$$

From (7) it's clear that if $|\mathrm{v}_{pk}^t|$ exceeds a positive constant value V_{max} specified by the user, the pth particle' velocity of kth user is assigned to be $\mathrm{sign}(\mathrm{v}_{pk}^t)V_{max}$, i.e. particles velocity on each of K-dimension is clamped to a maximum magnitude V_{max}. Besides, if the search space could be defined by the bounds $[P_{min}; P_{max}]$, then the value of V_{max} typically is set so that $V_{max}=\tau(P_{max}-P_{min})$, where $0.1 \le \tau \le 1.0$; please refer to Chapter 1 within the definition of reference [35].

In order to elaborate further about the inertia weight it can be noted that a relatively larger value of ω is helpful for global optimum, and lesser influenced by the best global and local positions, while a relatively smaller value for ω is helpful for convergence, i.e., smaller inertial weight encourages the local exploration as the particles are more attracted towards $\mathbf{b}_p^{best}$ and $\mathbf{b}_g^{best}$ [31, 32]. Hence, in order to achieve a balance between global and local search abilities, a linear inertia weight decreasing with the algorithm convergence evolving was adopted, which has demonstrated good global search capability at beginning and good local search capability latter iterations:

$$\omega[t]=(\omega_{initial}-\omega_{final})\bullet\left(\frac{\mathsf{G}-t}{\mathsf{G}}\right)^m+\omega_{final} \tag{8}$$

where $\omega_{initial}$ and ω_{final} is the initial and final weight inertia, respectively, $\omega_{initial} > \omega_{final}$, G is the maximum number of iterations, and $m \in [0.6;\ 1.4]$ is the nonlinear index [36].

3.3.2. Optical code path resource allocation optimization

The following maximization cost function could be employed as an alternative to OCP resource allocation optimization [33]. This single-objective function was modified in order to incorporate the near-far effect [37], [38]

$$J_1(\mathbf{p}) = \max \begin{array}{c} \frac{1}{K} \sum_{k=1}^{K} \mathsf{F}_k^{th}\left(1 - \frac{p_k}{P_{max}}\right) + \frac{\rho}{\sigma_{rp}} \\ \gamma_k \geq \gamma_k^*,\ \ 0 < p_k^l \leq P_{max},\ \ \ R^l = R_{min}^l\ \forall\ k \in K_l,\ and\ \forall\ l = 1,2,\ \dots,\ L \end{array} \tag{9}$$

where L is the number of different group of information rates allowing in the system, and K_l is the number of user in the lth rate group with minimum rate given by R_{min}^l. Important to say, the second term in eq. (9) gives credit to the solutions with small standard deviation of the normalized (by the inverse of rate factor, F^l) received power distribution:

$$\sigma_{rp}^2 = \mathrm{var}\left(F^1 p_1 G_{11},\ F^1 p_2 G_{22},\ \dots,\ F^l p_k G_{kk},\ \dots,\ F^L\ p_k G_{kk}\right) \tag{10}$$

i.e. the more close the normalized received power values are with other (small variance of normalized received power vector), the bigger contribution of the term $\frac{\rho}{\sigma_{rp}}$. For single-rate systems, $F^1 = \dots = F^l = \dots = F^L$. It is worth to note that since the variance of the normalized received power vector, σ_{rp}^2, normally assumes very small values, the coefficient ρ just also take very small values in order to the ratio $\frac{\rho}{\sigma_{rp}}$ achieves a similar order of magnitude of the first term in (9), been determined as a function of the number of users, K. Hence, the term $\frac{\rho}{\sigma_{rp}}$ has an effective influence in minimizing the near-far effect on OCDM/WDM systems, and at the same time it has a non-zero value for all swarm particles [33]. Finally, the threshold function in (9) is simply defined as:

$$\mathsf{F}_k^{th} = \begin{cases} 1, & \gamma_k \geq \gamma^* \\ 0, & otherwise \end{cases} \tag{11}$$

where the SNIR for the kth user, γ_k, is given by (2). The term $1 - \frac{p_k}{P_{max}}$ gives credit to those solutions with minimum power and punishes others using high power levels [33].

The PSO algorithm consists of repeated application of the updating velocity and position, eq. (5) and (6), respectively. The pseudo-code for the single-objective continuous PSO power allocation problem is presented in Algorithm 1.

Algorithm 1 Continuous PSO Algorithm for the Power Allocation Problem

---

Input: $\mathcal{P}, \mathcal{G}, \omega, C_1, C_2, V_{max}, R_{\min}$;   Output: $\mathbf{p}^*$

begin

1. initialize the population at $t = 0$;

    $\mathbf{B}[0] \sim U[P_{min}; P_{max}]$

    $\mathbf{b}_p^{best}[0] = \mathbf{b}_p[0] \ and \ \mathbf{b}_g^{best}[0] = \mathbf{p}_{max}$;

    $\mathbf{v}_p[0] = 0$: null initial velocity;

2. while $t \le \mathcal{G}$

    a. calculate $J(\mathbf{b}_p[t]), \forall \mathbf{b}_p[t] \in \mathbf{B}[t]$, using (9);

    b. update velocity $\mathbf{v}_p[t], p = 1, \dots, \mathcal{P}$, through (5);

    c. update best positions:

    for $p = 1, \dots, \mathcal{P}$

    If $J(\mathbf{b}_p[t]) < J(\mathbf{b}_p^{best}[t]) \ \& \ R_p[t] \ge R_{\min}$,

    $\mathbf{b}_p^{best}[t + 1] \leftarrow \mathbf{b}_p[t]$

    else $\mathbf{b}_p^{best}[t + 1] \leftarrow \mathbf{b}_p^{best}[t]$

    end

    if $\exists \mathbf{b}_p[t] \quad | \quad \left[J(\mathbf{b}_p[t]) < J(\mathbf{b}_g^{best}[t])\right] \ \& \ R_p[t] \ge R_{\min} \ \& \ \left[J(\mathbf{b}_p[t]) \le J(\mathbf{b'}_p[t]), \forall p' \ne p\right]$

    $\mathbf{b}_g^{best}[t + 1] \leftarrow \mathbf{b}_p[t]$

    else $\mathbf{b}_g^{best}[t + 1] \leftarrow \mathbf{b}_g^{best}[t]$

    d. Evolve to a new swarm population $\mathbf{B}[t + 1]$, using (9);

    e. Set $t = t + 1$.

    end

3. $\mathbf{p}^* = \mathbf{b}_g^{best}[\mathcal{G}]$.

end

$\mathcal{P}$: population size.

$\mathbf{B} = [\boldsymbol{b}_1, \dots, \boldsymbol{b}_p, \dots, \boldsymbol{b}_{\mathcal{P}}]$ particle population matrix, dimension K x $\mathcal{P}$.

$\mathcal{G}$: maximum number of swarm iterations.

$\mathbf{p}_{max}$: maximum power vector considering each mobile terminal rate class.

$R_{\min}$: minimum data rate common to all users

The quality of solution achieved by any iterative resource allocation procedure could be measured by how close to the optimum solution is the found solution, and can be quantified by the normalized mean squared error (NMSE) when equilibrium is reached. For power allocation problem, the NSE definition is given by,

$$NMSE[t] = \mathsf{E}\left[\frac{\|\mathbf{p}[t] - \mathbf{p}^*\|^2}{\|\mathbf{p}^*\|^2}\right] \qquad (12)$$

where $\| \bullet \|^2$ denotes the squared Euclidean distance to the origin, and $\mathsf{E}[\bullet]$ the expectation operator.

3.3.3. Energy efficiency optimization in OCPs

Recent studies have showed the importance of the consideration of energy consumption in optical communications design [39], considering the transmission infrastructure (transmitters, receivers, fibers and amplifiers) [40] and network infrastructure (switchers and routers) [41] aspects. Researches in a global scale network have indicated that the energy consumption of the switching infrastructure is larger than the energy consumption of the transport infrastructure [39-41]. In this context, it is necessary to improving the energy efficiency of switching and optimizing the network design in order to reduce the quantity of switching and overheads. The energy necessary for 1 bit transmission on each OCP can be expressed as [40],

$$E_i = p_i T_{bit} \quad \left[J/bit \right], i = 1,.., K \tag{13}$$

where $T_{bit} = 1/R$ is the time to transmit one bit over the network, with R is the bit rate. In our analysis, to determinate the energy is necessary define the individual OCPs transmitted power (p_i). The p_i is obtained by power control PSO algorithm given in Algorithm 1 and may be associated to a specific QoS, SNIR and maximum BER tolerated by the i-th optical node. In a power control situation, each optical node adjusts its transmitter power in an attempt to maximize the number of transmitted bits with minimum consumption of energy. This concept is formulated by the energy efficiency [42]:

$$\eta_i = \frac{R \cdot g(\gamma_i)}{p_i}, \quad i = 1,.., K \tag{14}$$

where $g(\gamma_i) = 1 - BER_i$ is the efficiency function, which represents the number of correct packets received for the for the i-th node, given a SNIR γ_i. In the same way this concept is used in a metric called *utility* that is the number of bits received per energy expended or the relation of the throughput and power dissipation [41].

For each i-th OCP, the maximum number of transmitted bits occurs at power level for which the partial derivative of energy efficiency function in (14) with respect to p_i is zero $\partial \eta_i / \partial p_i = 0$. Considering a SNIR general formula for CDMA networks, given by [6]

$$\gamma_i = \frac{h_{ii} p_i}{I_i + N_i}, i = 1,.., K \tag{15}$$

where h_{ij} are the total loss in the path that connects i-th transmitter node to j-th receiver node, I_1 is the interference from the others transmitters nodes and N_i is the receiver noise. We can obtain the derivative of energy efficiency referring to efficiency function and (15),

$$\frac{\partial \eta_i}{\partial p_i} = \frac{R}{p_i^2}\left(\gamma_i \frac{\partial g(\gamma_i)}{\partial \gamma_i} - g(\gamma_i)\right), i = 1,..,K \tag{16}$$

From (16) we observe, for $p_i > 0$, the necessary condition to maximize the energy efficiency is

$$\gamma_i \frac{\partial g(\gamma_i)}{\partial \gamma_i} - g(\gamma_i) = 0, i = 1,..,K \tag{17}$$

To satisfy (17) it is necessary that the received node achieves the target SNIR, namely γ_i^*. In this context, we propose the utilization of PSO power allocation algorithm in order to establish the lower energy per bit according to the OCDM/WDM network QoS requirements.

4. Numerical results

For all simulations, it is considered the transmission over a nonzero-dispersion shifted fiber (NFD)-ITU G.655 with fiber attenuation (α) of 0.2 dB/km, non-linear parameter (Γ) of 2 (W.km)$^{-1}$, zero-dispersion wavelength (λ_0) of 1550 nm, dispersion slope (S_0) of 0.07 ps/(nm^2.km). The signal is placed at λ_0 and its peak power is P. Note that the nonlinear length [24] $L_{NL} = 1/(\Gamma P)$ is limited to 500 km, which is much longer than the considered fiber lengths; besides self-phase modulation (SPM) should not seriously affect the system performance. Furthermore, the threshold power for stimulated Brillouin scattering (SBS) is below a few mW; as a result, SBS should also not interfere in our results. Similarly, for these considerations, the physical impairments, such as stimulated Raman scattering (SRS) should not be relevant [24]. Typical parameter values for the noise power in all optical amplifiers were assumed [21]. So, it was adopted $n_{SP} = 2$, $h = 6.63 \times 10-34$ (J/Hz), $f = 193.1$ (THz), $G = 20$ (dB) and $B_0 = 30$ (GHz). Herein, it was considered an amplifier gain of 20 dB with a minimum spacing of 60 km, $D_{PMD} = 0.1 ps/\sqrt{km}$, and $D = 15$ ps/nm/km. Losses for encoder/decoder and router architecture of 5 dB and 20 dB, respectively, were included in the power losses model [22-24]. The parameters are code weight of 4 and code length of 101, thus the code is characterized by (4 × 101, 4, 1,0) and the target SNIR $\gamma_i^* = 20$dB was adopted.

4.1. PSO parameters optimization for resource allocation problem

For power resource allocation problem, simulation experiments were carried out in order to determine the suitable values for the PSO input parameters, such as acceleration coefficients, C_1 and C_2, maximal velocity factor, V_{max}, weight inertia, ω, and population size, P, regarding the power optimization problem.

The continuous optimization for resource allocation problem was investigated in [33], [34], it indicates that after an enough number of iterations (G) for convergence, the maximization of

cost function were obtained within low values for both acceleration coefficients. The V_{max} factor is then optimized. The diversity increases as the particle velocity crosses the limits established by $[\pm V_{max}]$. The range of V_{max} determines the maximum change one particle can take during iteration. With no influence of inertial weight ($\omega = 1$), it was obtained that the maximum allowed velocity V_{max} is best set around 10 to 20% of the dynamic range of each particle dimension [33]. The appropriate choose of V_{max} avoids particles flying out of meaningful solution space. Herein, for OCP power allocation problem, similar to the problem solved in [33], the better performance *versus* complexity trade-off was obtained setting the maximal velocity factor value as $V_{max} = 0.2 \, (P_{max} - P_{min})$. For the inertial weight, ω, simulation results has confirmed that high values imply in fast convergence, but this means a lack of search diversity, and the algorithm can easily be trapped in some local optimum, whereas a small value for ω results in a slow convergence due to excessive changes around a very small search space. In this work, it was adopted a variable ω, as described in (8), but with $m = 1$, and initial and final weight inertia setting up to $\omega_{initial} = 1$ and $\omega_{final} = 0.01$. Hence, the initial and final maximal velocity excursion values were bounded through the initial and final linear inertia weight multiplied by V_{max}, adopted as a percentage of the maximal and minimal power difference values [33],

$$\omega_{initial} \bullet V_{max} = 0.2 \, (P_{max} - P_{min}) \quad \omega_{final} \bullet V_{max} = 0.002 \, (P_{max} - P_{min}) \tag{18}$$

Finally, stopping criterion can be the maximum number of iterations G (velocity changes allowed for each particle) combined with the minimum error threshold:

$$\left| \frac{J[t] - J[t-1]}{J[t]} \right| < \epsilon_{stop} \tag{19}$$

where typically $\epsilon_{stop} \in [0.001; 0.01]$. Alternately, the convergence test can be evaluated through the computation of the average percent of success, taken over T runs to achieve the global optimum, and considering a fixed number of iterations G. A convergence test is considered 100% successful if the following relation holds:

$$|J|G| - J|\mathbf{p}^*|| < {}_1 J[\mathbf{p}^*] + {}_2 \tag{20}$$

where, $J|\mathbf{p}^*|$ is the global optimum of the objective function under consideration, $J|G|$ is the optimum of the objective function obtained by the algorithm after G iterations, and ϵ_1, ϵ_2 are accuracy coefficients, usually in the range $[10^{-6}; 10^{-2}]$. In this study it was assumed that T = 100 trials and $\epsilon_1 = \epsilon_2 = 10^{-2}$.

The parameter ρ in cost function (9), was set as a function of the number of users OCPs (K), such that $\rho = K \times 10^{-19}$. This relation was adapted from [38] for the power-rate allocation

problem through non-exhaustive search [33]. The swarm population size was set by $P = K + 2$.

In power resource allocation problem for access network systems the parameters optimization, mainly acceleration coefficients C_1 and C_2, depend on the number of simultaneous transmitted users [16], [33]. In the case of realistic OCDM/WDM routed networks, the number of simultaneous transmitted OCPs is low, generally around or less than 10 [2], [5], [6], [25]. Fast convergence without losing certain exploration and exploitation capabilities could be obtained with optimization of acceleration parameters in relation to the standard values adopted in the literature [16]. Previous works have shown that the best convergence *versus* solution quality trade-off was achieved with $C_1 = 1$ and $C_2 = 2$ for number of codes less than 10 [16], [33]. On the other hand, the classical value adopted are $C_1 = C_2 = 2$ [32-35]. In this context, simulation experiments were carried out in order to determine the good choice for acceleration coefficients C_1 and C_2 regarding the power optimization problem. Fig. 4 illustrates different solution qualities in terms of the normalized mean squared error (NMSE), when different values for C_1 combining with $C_2 = 2$ in a system with number of OCPs equal to 7, considering 1 span. Previous simulations have shown the non poor convergence for different value of C_2 [33].The lengths of OCPs are uniformly distributed between 2 and 100 km. The NMSE values where taken as the average over T = 100 trials. Besides, the NMSE convergence values were taken after G = 800 iterations.
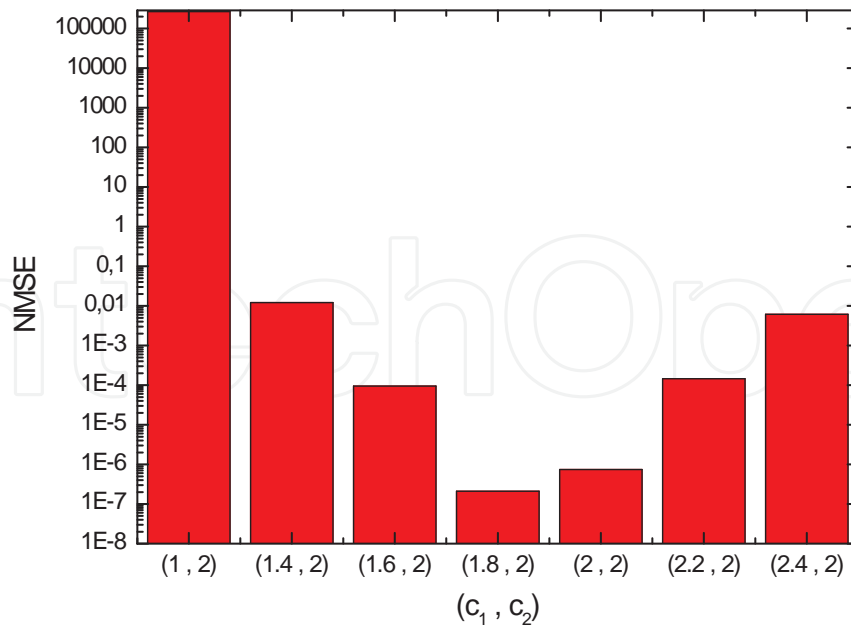

Figure 4. Normalized mean squared error (NMSE) for different values for C_1 combining with $C_2 = 2$ in a system with number of OCPs equal to 7, considering 1 span.

Numerical results have shown the solution quality for different values of acceleration coefficient C_1 and it was found $C_1 = 1.8$ presents the lower NMSE for the number of OCPs < 10. Hence, the best solution quality was achieved with $C_1 = 1.8$ and $C_2 = 2$. Fig. 5 shows the sum of power for the evolution through the $t=1,\ldots, 800$ iterations for 7 OCPs under different acceleration value of C_1 and $C_2 = 2$, considering 1 span.
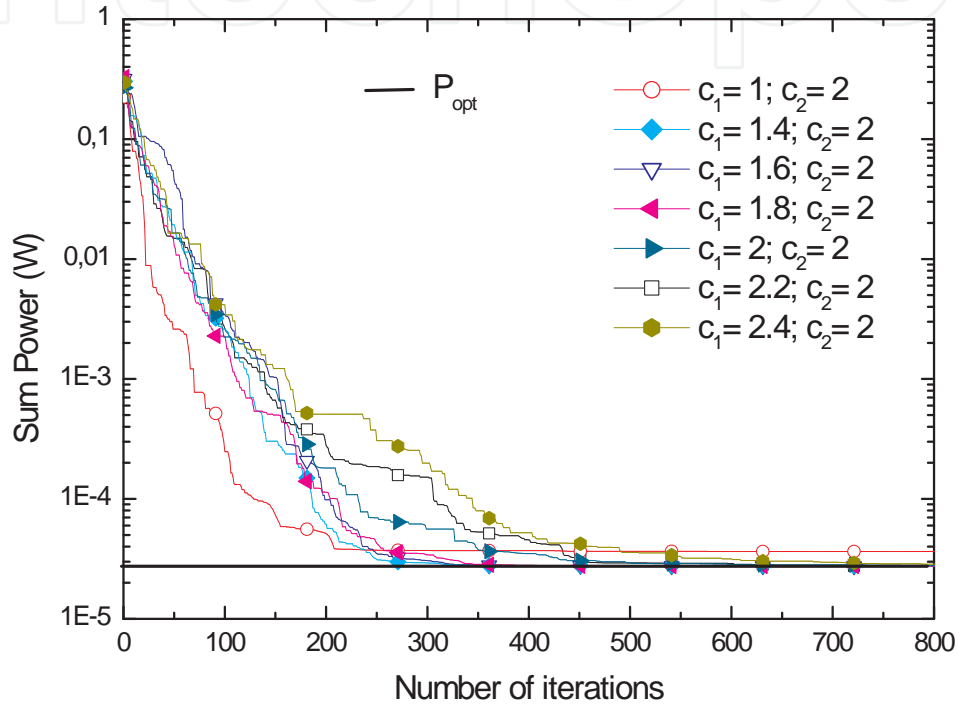

Figure 5. Sum of power for power vector evolution through the 800 iterations for 7 OCPs under different acceleration value of C_1 and $C_2 = 2$ for 1 spans.

The algorithm reaches convergence for $C_1 = 1.4, 1.6, 1.8, 2, 2.2$ and 2.4, however it doesn't reach acceptable convergence for $C_1 = 1$. Simulations revealed that increasing parameter C_1 results in a slower convergence with approximately 320, 343, 373, 639, 659 and 713, iterations, respectively. However, NMSE for faster convergence is higher than for the slower convergence parameters with minimum value for $C_1 = 1.8$, as indicated in Fig. 4. In this context, the best convergence *versus* solution quality trade-off was achieved with $C_1 = 1.8$ and $C_2 = 2$ for number of OCPs of 7.

It is worth to expand this analysis to other number of OCPs that are generally between 4 and 8 OCPs. For this purpose, Fig 6 shows the NMSE for the number of OCPs regarding two combination of acceleration coefficient: i) optimized herein ($C_1 = 1.8$ and $C_2 = 2.0$) and reported in the literature ($C_1 = 2.0$ and $C_2 = 2.0$).
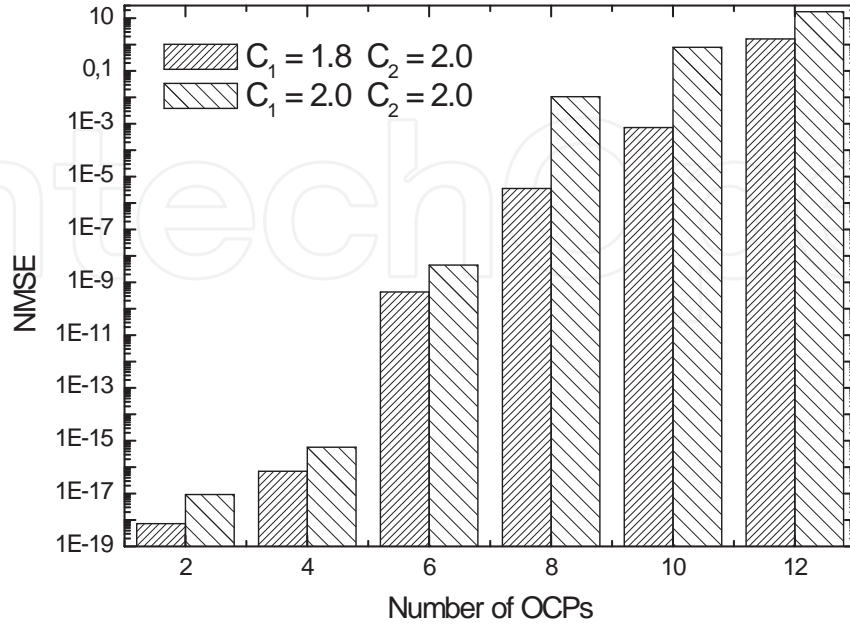
Figure 6. Normalized mean squared error (NMSE) for the number of OCPs for (C_1 = 1.8 and C_2 = 2.0) and (C_1 = 2.0 and C_2 = 2.0), considering 1 span.

The OCPs increasing affects the solution quality. This effect is directly related to the MAI rising which increases with the number of OCPs, i.e., the MAI effects are strongly influenced by the increase of the active OCPs; an error occurs when cross-correlational pulses from the $(K-1)$ interfering optical code paths built up to a level higher than the autocorrelation peak, changing a bit zero to a bit one.

In conclusion, our numerical results for the power minimization problem have revealed for low system loading that the best acceleration coefficient values lie on C_1 = 1.8 and C_2 = 2.0, in terms solution quality trade-off. This result was compared with C_1 = 2.0 and C_2 = 2.0 previously reported in the literature [32]-[35].

4.2. PSO optimization for OCPs

The solution quality *versus* convergence trade-off analysis presented in Figs. 4, 5 and 6 for the PSO's acceleration coefficients optimization in the case of OCDM/WDM networks with 1 span should be extended taking into account the use of more spans. The state-of-art for the number of spans without electronic regeneration is around 4 considering the ASE effect limiting applying fibers with low PMD effects for bit rate of 10 Gbps (lower than 40 Gbps) [29]. In Fig. 7 the analysis of subsection 4.1 is extended until 8 spans, showing the influence of the number of spans on the NMSE for 7 OCPs and the same parameters values optimized in that subsection.
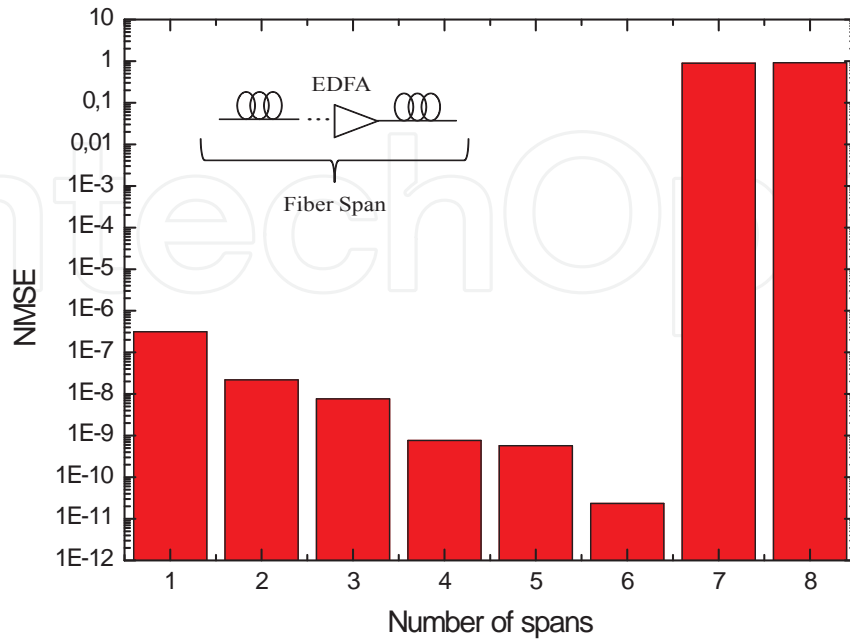
Figure 7. NMSE for the number of spans for 7 OCPs.

The results show that NMSE decreases when the number of spans increases until 6 spans, after this number of spans the NMSE alters the tendency and increases. This behavior shows the limitation of PSO convergence when the ASE increases. After 6 spans the PSO algorithm does not reach the total convergence. This fact occurs, directly by the limitations generate with the increase of the ASE. In other sense, the transmitted power needed to reach the target SNIR will overcome the maximum allowed transmitted power. The average number of spans increases slightly as K increases, as longer OCP routes become available. This increase is, however, not very significant, and on average, the path lengths are around four spans [22].

The convergence quality of the PSO algorithm presents variation with the increase in the number of spans. The figure of merit utilized as tool to this analysis is the rate of convergence (RC), which can be described as the ratio of PSO solution after the t-th iteration divided by the PSO solution after total convergence, which in this optimization context is given by the matrix inversion solution, as discussed in Section 3.1. Recalling eq. (19), the RC can be expressed in term of ϵ_{stop} as:

$$RC[t] = 1 - \left| \frac{J[t] - J[\mathbf{p}^*]}{J[\mathbf{p}^*]} \right| \tag{21}$$

The reader interested in quality of solution metrics, a similar definition for RC and another figure of merit for the PSO, namely success cost, are presented in [35].
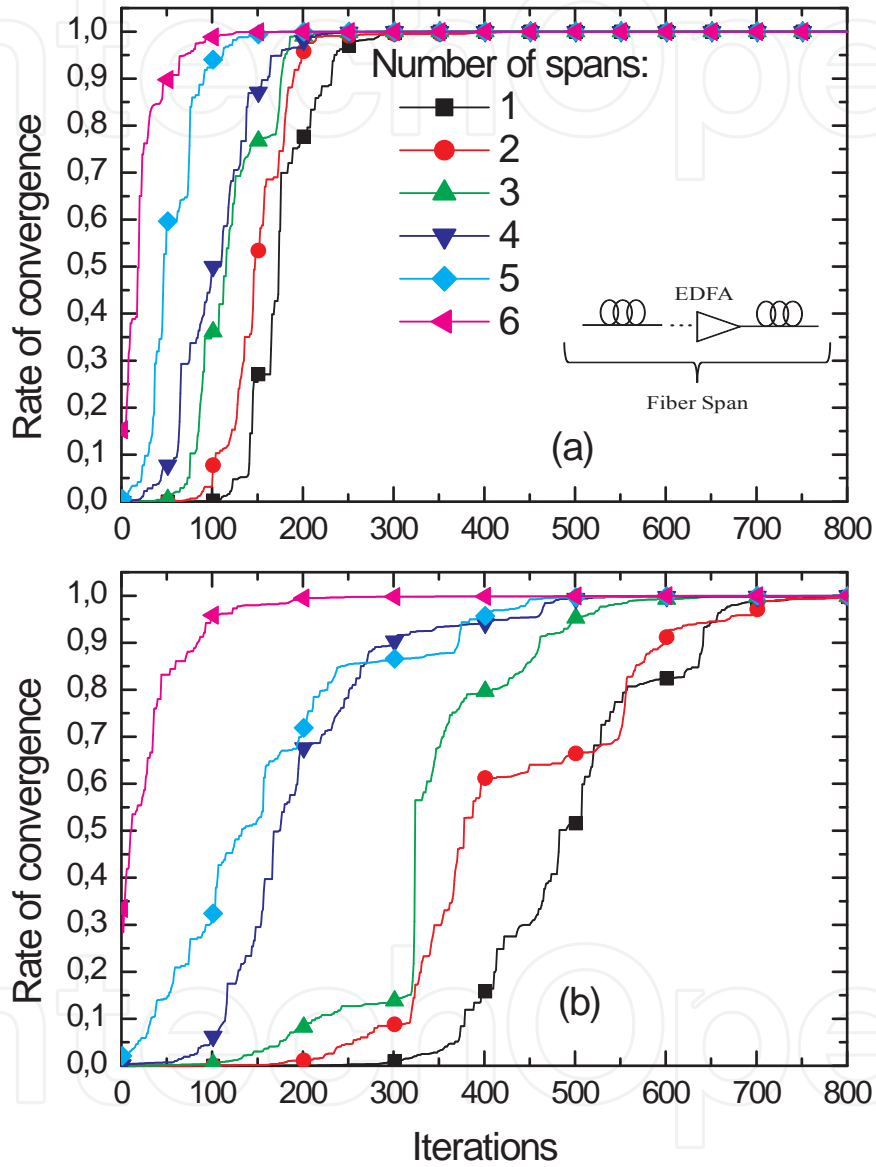

Figure 8. Rate of convergence versus the number of iterations for 1 until 6 spans for (a) 4 OCPs and (b) 8 OCPs.

Fig. 8 (a) and (b) shows the convergence rate of the sum of power for vector evolution through the 800 iterations for 4 a 8 OCPs, respectively, considering 1 until 6 spans. The results have shown that increasing span number results in a faster convergence. This fact occurs because until 6 spans the increase of the number of span increases the contribution of

the amplifier with signal, besides for more than 6 spans the contribution of the amplifier is for the ASE noise. On the other hand, the increase in the number of OCPs results in a slow convergence that results from the MAI between the OCPs.

In summary, our numerical results for the power minimization problem considering different number of spans have revealed the viability of the PSO algorithm deployment to solve a power allocation in OCPs with until 6 spans in order to guarantee the solution quality in terms of NMSE. Furthermore, the numerical results revealed that increasing the number of spans results in a faster convergence. In this context, the PSO algorithm is quite suitable to solve a power allocation in OCPs that presents an average of 4 spans as reported in the literature [22].

In order to evaluate the impact of physical restrictions on the OCM/WDM network, further numerical results presented in Fig. 9 shows the sum power evolution of the PSO algorithm with respect to the number of iterations, considering a) 4 OCPs, and b) 8 OCPs. One span was considered as reference for bit rate of 10 Gbps taking into account two situations: i) with only ASE effects, ii) with ASE, GVD and PMD effects.

The target SNIR established for all the nodes is equal, and if the perfect power balancing with ideal physical layer (no physical impairments) is assumed, it could be demonstrated that the maximum SNIR and the transmitted power are defined by the number of OCPs in the same route. However, when the ASE, GVD and PMD effects are considered, there is a penalty. This penalty represents the received power reduction due to temporal spreading. Fig. 9 shows that when ASE, GVD and PMD effects are considered there is a power penalty of 3 decades compared with the situation where only ASE is considered (fibers with low PMD). Comparing Figs. 9(a) and 9(b), it could be noticed that the convergence velocity depends on the number of OCPs. The increase of OCPs from 4 to 8 affects the convergence velocity, from ≈200 to ≈500 iterations, respectively. This effect is directly related to the MAI increasing, which increases with the number of OCPs. The MAI effects are strongly influenced by the increase of the active number of OCPs; as explained before, an error occurs when cross-correlational pulses from the $(K - 1)$ interfering optical code paths built up to a level higher than the autocorrelation peak, changing a bit zero to a bit one. The PMD effects degrade the performance when the link length and bit rate increase. This effect occurs because PMD impairment establishes an upper bound on the link length, which causes the temporal spreading of optical pulses. The upper bound for link distance depends on the chip-rate distance product $(d.R.N_T)$, where d is the link length, R is the bit rate, and N_T is the code length. The analysis of code parameters, MAI and PMD effects for 2D-based OCPs was previously reported in [20].

In OCDM/WDM networks, the OCPs with various classes of QoS are obtained with transmission of different power levels. Distinct power levels are obtained with adjustable transmitters and it does not cause the change of the bit rate. The intensity of the transmitted optical signal is directly adjusted from the laser source with respect to the target SNIR by PSO algorithm. Table 1 shows the optimization aspects of QoS regarding different levels of SNIR considering sum power and NMSE for 4 and 8 OCPs with 1 span.
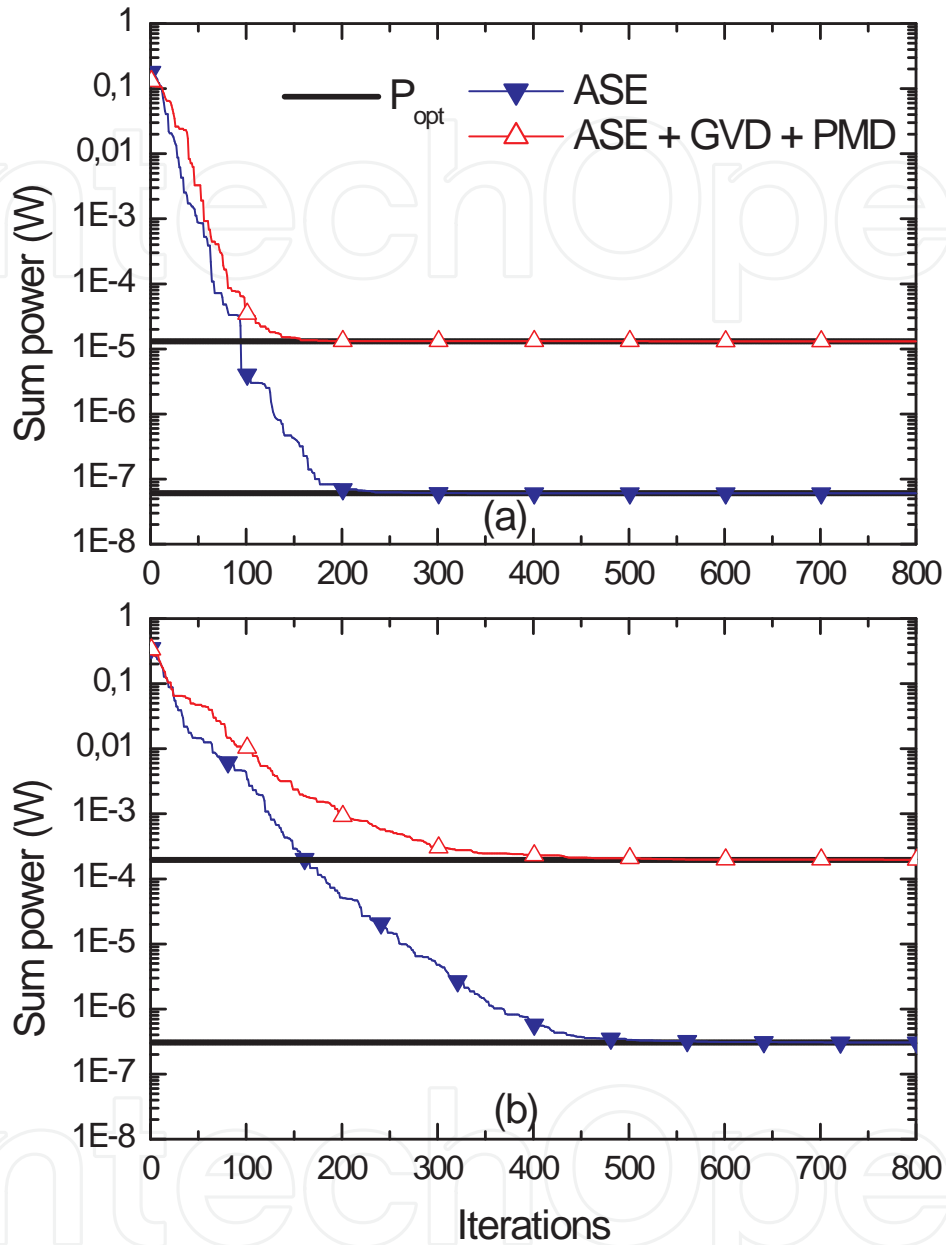
Figure 9. PSO sum power evolution for a) 4 OCPs; b) 8 OCPs. One span as reference, with R=10 Gbps. Two situations: i) ASE effects, ii) ASE, GVD and PMD effects.

The results in Table I show the necessary values for transmitted power, as well as the solution quality evaluation in terms of NMSE. The increase in the target SNIR results in the increase of the transmitted power, which is major for more OCPs. On the other hand, the solution quality (NMSE) decreases with the increase of SNIR target, since the number of the PSO iterations is fixed.

		4 OCPs		8 OCPs	
SNIR (dB)	BER	Sum power (W)	NMSE	Sum power (W)	NMSE
17	7.2×10^{-13}	3.3×10^{-8}	3.0×10^{-18}	1.2×10^{-7}	2.3×10^{-8}
20	7.6×10^{-24}	6.0×10^{-8}	6.2×10^{-16}	2.8×10^{-7}	1.2×10^{-3}
22	1.2×10^{-36}	9.5×10^{-8}	3.8×10^{-16}	4.3×10^{-7}	1.0×10^{-1}

Table 1. The optimization aspects of QoS.

4.3. PSO optimization for energy efficiency in OCPs

An efficient resource allocation algorithm is needed to overcome the problem of energy efficiency and to enhance the performance and QoS of the optical network. This could be achieved via signal-to-noise plus interference (SNIR) PSO optimization.
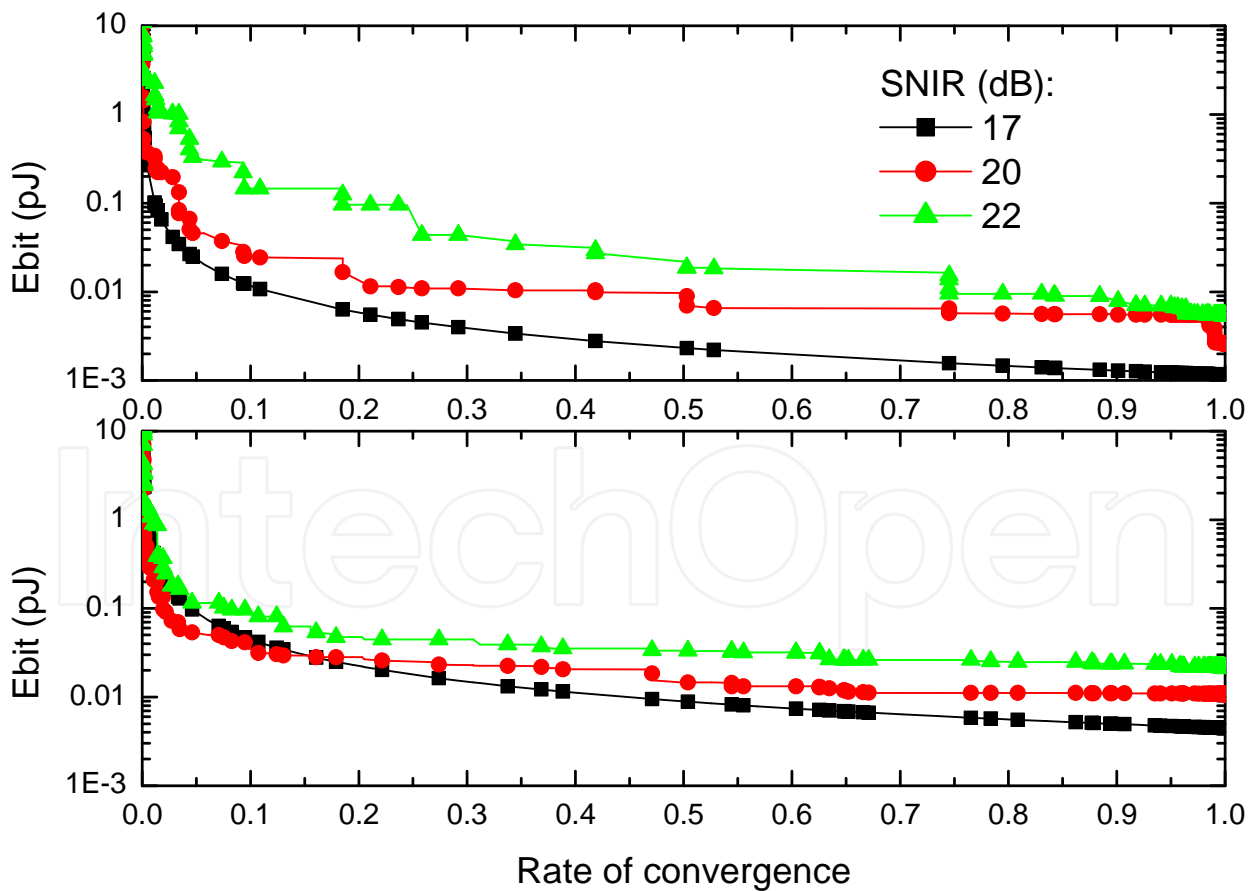

Figure 10. Energy per bit sum of the OCPs as a function of the rate of convergence using PSO algorithm. Three different SNIRs target of 17, 20 and 22 dB; a) 4 OCPs and b) 8 OCPs.

Fig. 10 shows the sum of energy per bit as a function of the rate of convergence of eq. (21) for the PSO optimization with different QoS requirements represented by SNIR target of 17, 20 and 22 dB, considering a) 4 OCPs and b) 8 OCPs, i.e., same scenario presented in the previous subsection. One can see when rate of convergence evolving, the energy per bit solution offered by the PSO algorithm convergences to the best lower values as predicted in (17).

It can be seen from Fig. 10 the impact of the PSO power allocation optimization procedure (in terms of transmitted energy per bit) on the energy efficiency improvement. The deployment of PSO with 100% of rate of convergence results in an enormous saving of energy. Indeed, with very low number of PSO iterations, rate of convergence is poor ($RC < 0.03$), the transmitted energy per bit is high because the MAI are strongly influenced by near-far effects. As expected, the increase of the active OCPs from 4 to 8, results in the increase of the transmitted energy per bit to reach the SNIR target. Furthermore, one can analyze the variation of saving energy for different levels of convergence rate; for instance, the variation of saving energy regarding the rate convergence in the range $RC \in [0.5; 1.0]$ remains in approximately from 40 to 60 % for different SNIR target and number of OCPs, as presented in Fig. 10. In this context, aiming to analyze the effect of the number of spans in the transmitted energy per bit for 4 and 8 OCPs, Table 2 presents the sum energy per bit considering SNIR target of 20 dB and rate of convergence of 0.5 and 1.0, for 2 and 4 spans.

	4 OCPs		8 OCPs	
Number of spans	Σ energy (pJ) RC=0.5	Σ energy (pJ) RC=1.0	Σ energy (pJ) RC=0.5	Σ energy (pJ) RC=1.0
2	0.0135	0.0120	0.3145	0.1100
4	1.0545	1.0108	2.2295	1.8199

Table 2. Sum energy per bit in [pJ] for SNIR target of 20 dB.

The results show the impact of the number of spans in the transmitted energy per bit for the variation of rate convergence of 0.5 and 1. As expected, the increase in the number of spans and the number of OCPs results in the increase of the transmitted energy per bit. Besides, the sum energy per bit variation, regarding the RC from 0.5 to 1.0, declines with the increase of the number of spans from 2 to 4. This results agree with the previous results illustrated in Fig. 8, meaning the increase of the number of spans accelerate the RC.

5. Conclusions

In this chapter, optimization procedures based on particle swarm intelligence are investigated in details, aiming to efficiently solve the optimal resource allocation for signal-to-noise plus interference ratio (SNIR) optimization of optical code paths (OCPs) from OCDM/WDM networks under quality of service (QoS) restrictions and energy efficiency constraint prob-

lem, considering imperfections on physical constraints. The SNIR model considers multiple access interference (MAI) between the OCP based on 2-D codes (time/wavelength), amplifier spontaneous emission (ASE) at cascaded amplified spans, and group velocity dispersion (GVD) and polarization mode dispersion (PMD) dispersion effects. The characteristic of the particle swarm optimization (PSO) is attractive due their performance-complexity tradeoff and fairness regarding the optimization methods that use numerical methods, matrix inversion and other heuristics. The resource allocation optimization based on PSO strategy allows the regulation of the transmitted power and the number of active OCPs in order to maximize the aggregate throughput of the OCDM/WDM networks considering QoS and energy efficiency constraint. For the network optimization context, system model was described, figures of merit were presented and a suitable model of PSO was developed, with emphasis in the optimization of input parameters and network performance. Afterward, extensive numerical results for the optimization problem are discussed taking into account realistic networks operation scenarios.

In order determine the suitable values for the PSO input parameters, such as acceleration coefficients, C_1 and C_2, maximal velocity factor, V_{max}, weight inertia, ω, and population size, P, simulation experiments were carried out in regarding the power optimization problem for OCDM/WDM networks. In these networks, the number of simultaneous transmitted OCPs is low, generally around or less than 10. For our specific problem, the optimized input parameters are different from the reported in the literature for similar problems. The numerical results considering the number of spans have revealed the viability of the PSO algorithm deployment in order to solve a power allocation in OCPs with until 6 spans to guarantee the solution quality and convergence. This result is adequate considering the average of 4 spans without electronic regeneration presented for this kind of network. Besides, the numerical results have shown a penalty when the ASE, GVD and PMD effects are considered. This penalty represents the received power reduction due to temporal spreading. Indeed, when ASE, GVD and PMD effects are considered there is a power penalty of 3 decades compared with the situation where only ASE is considered (fibers with low PMD). Finally, our numerical results reveal considerable variation of transmitted energy for different levels of convergence rate of PSO algorithm, in which the maximum energy efficiency is reached when the convergence of PSO algorithm is total. Interesting, even with only 10%-20% of the total PSO convergence, the network is able to operate within a remarkable energy efficiency gain region compared to network operation without power allocation policy.

Author details

Fábio Renan Durand[1], Larissa Melo[1], Lucas Ricken Garcia[1], Alysson José dos Santos[2] and Taufik Abrão[2]

1 Federal University of Technology, Parana, Campo Mourão, Brazil

2 State University of Londrina – Electrical Engineering Department, Brazil

References

[1]   E. Wong, "Next-Generation Broadband Access Networks and Technologies," Journal of Lightwave Technology, vol. 30, no. 4, pp. 597 – 608, Feb., 2012

[2]   H. Beyranvand and J. Salehi, "All-optical multiservice path switching in optical code switched GMPLS core network", Journal of Lightwave Technology, vol. 27, no. 17, pp. 2001 – 2012, Jun. 2009.

[3]   H. Yin and D. J. Richardson, Optical code division multiple access communication networks: theory and applications. Berlin: Springer-Verlag and Tsinghua University Press, 2009.

[4]   A. Rahbar, "Review of Dynamic Impairment-Aware Routing and Wavelength Assignment Techniques in All-Optical Wavelength-Routed Networks", IEEE Communications Surveys & Tutorials, ACCEPTED FOR PUBLICATION

[5]   F. R. Durand, M. Lima and E. Moschim, "Impact of pmd on hybrid wdm/ocdm networks," IEEE Photonics Technology Letters, vol. 17, no. 12, pp. 2787–2789, December 2005.

[6]   F. R. Durand and T. Abrão, "Distributed SNIR Optimization Based on the Verhulst Model in Optical Code Path Routed Networks With Physical Constraints", Journal of Optical Communications and Networking, vol. 3, no. 9, pp. 683–691, Sep. 2011. doi: 10.1364/JOCN.3.000683

[7]   F. R. Durand, M. S. Filho and T. Abrão, "The effects of power control on the optical CDMA random access protocol", Optical Switching and Networking, (In press) doi: 10.1016/j.osn.2011.06.002

[8]   N. Tarhuni, T. Korhonen, M. Elmusrati and E. Mutafungwa, "Power Control of Optical CDMA Star Networks", Optics Communications, vol. 259, pp. 655 – 664, Mar. 2006.

[9]   E. Inaty, R. Raad, P. Fortier, and H. M. H. Shalaby, "A Fair QoS-Based Resource Allocation Scheme For a Time-Slotted Optical OV-CDMA Packet Networks: a Unified Approach," Journal of Lightwave Technology, vol. 26, no. 21, pp. 1-10, Jan. 2009.

[10] E. Inaty, H. Shalaby, P. Fortie, and L. Rusch, "Optical Fast Frequency Hopping CDMA System Using Power Control", Journal of Lightwave Tech., vol. 20, n. 2, pp. 166 – 177, March 2003.

[11] C. C. Yang, J. F. Huang, and T. C. Hsu, "Differentiated service provision in optical CDMA network using power control," IEEE Photon. Technol. Lett., vol. 20, no. 20, pp. 1664–1666, 2008.

[12] S. Khaleghi and Mohammad Reza Pakravan, Quality of Service Provisioning in Optical CDMA Packet Networks, Journal of Optical Communications and Networking, vol. 2, no. 5, pp. 283–292, Feb. 2010.

[13] H. Yashima, and T. Kobayashi "Optical CDMA with time hopping and power control for multirate networks," J. Lightwave Technol., vol. 21, pp. 695-702, March 2003.

[14] T. Miyazawa and I. Sasase "Multi-rate and multi-quality transmission scheme using adaptive overlapping pulse-position modulator and power controller in optical network," IEEE ICON, vol. 1, pp. 127-131, November 2004.

[15] R. Raad, E. Inaty, P. Fortier, and H. M. H. Shalaby, "Optimal resource allocation scheme in a multirate overlapped optical CDMA system," J. of Lightwave Technol., vol. 25, no. 8, pp. 2044 – 2053, August 2007.

[16] M. Tang, C. Long and X. Guan, "Nonconvex Optimization for Power Control in Wireless CDMA Networks," Wireless Personal Communications, vol. 58, n. 4, pp. 851-865, 2011.

[17] Q. Zhu. and L. Pavel, "Enabling Differentiated Services Using Generalized Power Control Model in Optical Networks", IEEE Transactions on Communications, vol. 57, no 9, p. 1 – 6, Sept. 2009.

[18] R. Ramaswami, K. Sivarajan and G. Sasaki, Optical Networks: A Practical Perspective, Morgan Kaufmann, Boston, MA, 2009.

[19] E. Mutafungwa, "Comparative analysis of the traffic performance of fiber-impairment limited WDM and hybrid OCDM/WDM networks", Photon Network Commun., vol. 13, pp.53–66, Jan. 2007.

[20] F R. Durand, L. Galdino, L. H. Bonani, F. R. Barbosa1, M. L. F. Abbade and Edson Moschim, "The Effects of Polarization Mode Dispersion on 2D Wavelength-Hopping Time Spreading Code Routed Networks", Photonics Network Communications, vol. 20, no. 1, pp. 27 – 32, Aug. 2010. DOI 10.1007/s11107-010-0242-6.

[21] F. R. Durand, M. L. F. Abbade, F. R. Barbosa, and E. Moschim, "Design of multi-rate optical code paths considering polarisation mode dispersion limitations," IET Communications, vol. 4, no. 2, pp. 234–239, Jan. 2010.

[22] Camille-Sophie Brès and Paul R. Prucnal, "Code-Empowered Lightwave Networks", J. Lightw. Technol. , vol. 25, n. 10, pp. 2911 – 2921, Oct. 2007.

[23] Yue-Kai Huang, Varghese Baby, Ivan Glesk, Camille-Sophie Bres, Christoph M. Greiner, Dmitri Iazikov, Thomas W. Mossberg, and Paul R. Prucnal, Fellow, "Novel Multicode-Processing Platform for Wavelength-Hopping Time-Spreading Optical CDMA: A Path to Device Miniaturization and Enhanced Network Functionality", IEEE Journal of Selected Topics in Quantum Electronics, vol. 13, no. 5, pp. 1471 – 1479, september/october 2007.

[24] G. P. Agrawal, Fiber-optic communication systems, John Wiley & Sons, 2002.

[25] K. Kitayama and M. Murata, "Versatile Optical Code-Based MPLS for Circuit, Burst and Packet Switching", J. Lightwave Technol, vol. 21, no. 11, pp. 2573 – 2764, Nov. 2003.

[26] S. Huang, K. Baba, M. Murata and K. Kitayama, "Variable-bandwidth optical paths: comparison between optical code-labeled path and OCDM path", J. Lightwave Technol., vol. 24, no. 10, pp. 3563 – 3573, Oct. 2006.

[27] Kerim Fouli e Martin Maier, "OCDMA and Optical Coding: Principles, Applications, and Challenges", IEEE Communications Magazine, vol. 45, no. 8, pp. 27 – 34, Aug. 2007.

[28] G.-C. Yang and W.C. Kwong, Prime codes with applications to CDMA optical and wireless networks, Artech House, Boston, MA, 2002.

[29] G. Pavani, L. Zuliani, H. Waldman and M. Magalhães, "Distributed approaches for impairment-aware routing and wavelength assignment algorithms in GMPLS networks", Computer Networks, vol. 52, no. 10, pp. 1905–1915, July 2008.

[30] A. L. Sanches, J. V. dos Reis Jr. and B.-H. V. Borges, "Analysis of High-Speed Optical Wavelength/Time CDMA Networks Using Pulse-Position Modulation and Forward Error Correction Techniques", J. Lightwave Technol., vol. 27, no. 22, pp. 5134 – 5144, Nov. 2009.

[31] J. Kennedy and R.C. Eberhart, "Particle swarm optimization", in Proceedings of IEEE International Conference on Neural Networks, Piscataway, USA, pp. 1942–1948, 1995.

[32] N. Nedjah and L. Mourelle, Swarm Intelligent Systems, Springer, Springer-Verlag Berlin Heidelberg, 2006.

[33] T. Abrão, L. D. Sampaio, M. Proença Jr., B. A. Angélico and Paul Jean E. Jeszensky, Multiple Access Network Optimization Aspects via Swarm Search Algorithms, In: Nashat Mansour. (Org.). Search Algorithms and Applications. 1 ed. Vienna, Austria: InTech, ISBN 978-953-307-156-5, 2011, v. 1, p. 261-298.

[34] K. Zielinski, P. Weitkemper, R. Laur, and K. Kammeyer, "Optimization of Power Allocation for Interference Cancellation With Particle Swarm Optimization", IEEE Transactions on Evolutionary Computation, vol. 13, no. 1, pp. 128 – 150, Feb. 2009.

[35] N. Nedjah and L. M. Mourelle. Swarm Intelligent Systems, Springer, Springer-Verlag Berlin Heidelberg, 2006.

[36] A. Chatterjee and P. Siarry, Nonlinear inertia weight variation for dynamic adaptation in particle swarm optimization, Computers & Operations Research, vol 33, no. 3, pp. 859–871.

[37] M. Moustafa, I. Habib, and M. Naghshineh, Genetic algorithm for mobiles equilibrium, MILCOM 2000. 21st Century Military Communications Conference Proceedings 2000.

[38] H. Elkamchouchi, H., EIragal and M. Makar, Power control in cdma system using particle swarm optimization, 24th National Radio Science Conference, pp. 1–8. 2007.

[39] S. Yoo, "Energy Efficiency in the Future Internet: the Role of Optical Packet Switching and Optical Label Switching", IEEE J Selected Topics in Quantum Electronics, vol. 17, no. 2, pp. 406 – 418, March-April 2011.

[40] Rodney S. Tucker, "Green Optical Communications - Part I: Energy Limitations in Transport", IEEE J Selected Topics in Quantum Electronics, vol. 17, no. 2, pp. 245 – 260, March-April 2011.

[41] Rodney S. Tucker, "Green Optical Communications - Part II: Energy Limitations in Networks", IEEE J Selected Topics in Quantum Electronics, vol. 17, no. 2, pp. 261 – 274, March-April 2011.

[42] D. Goodman and Narayan Mandayan "Power control for wireless data", IEEE Personal Communications, vol. 7, no. 2, pp. 48 – 54, April 2000.